ELSEVIER

Journal of Magnetism and Magnetic Materials 164 (1996) 284–292

journal of magnetism and magnetic materials

Current status of our understanding of magnetotransport in magnetic multilayers

Peter M. Levy *, Shufeng Zhang

4 Washington Place, Physics Department, New York University, New York, NY 10003, USA

Received 13 May 1996; revised 7 July 1996

Abstract

We review the current theoretical understanding of giant magnetoresistance in magnetic multilayered structures. The active ingredients producing magnetoresistance for current *in* and *perpendicular* to the plane of the layers are discussed, and the effect of superlattice band structure on transport is reviewed. Differences between ballistic and diffusive electron transport are highlighted. The effective fields used to account for vertex corrections for current perpendicular to the layers is discussed and their meaning is defined.

Keywords: Magnetotransport; Magnetic multilayers; Giant magnetoresistance; Effective field

1. Introduction

The giant magnetoresistance (GMR) observed in the transition-metal magnetic multilayers results from the change in the scattering of the conduction electrons as the magnetic configuration of the multilayer goes from one where the layers are on the average antiparallel in zero or coercive field to one where they are aligned in parallel at the saturation field. There is some debate as to the origin of the dependence of this scattering on the magnetic configuration; however it is clear that spin dependent scattering is needed for GMR to occur, and that the scattering at interfaces plays a critical role in producing this effect.

From fits to GMR data on magnetic multilayers one arrives at two conclusions: that the strength, and that the spin dependence of the scattering at the interfaces between layers is stronger than in the bulk of the layers. That the scattering is larger at interfaces is not surprising, after all there is a rapid change in the electronic structure (potential step) in the interfacial region; the layers are not flat so that there is geometrical roughness and elements from one layer diffuse into the neighboring layer. Each of these aspects have received some attention; the 'band mismatch' between the dissimilar metals constituting the interface is a crude indicator of the strength of the scattering induced by roughness (geometrical and interdiffusional) [1]. Geometrical roughness produces an angular dependence to the scattering, i.e., the interfacial scattering is stronger for electron trajectories perpendicular to the plane of the layers [2]; and interfaces have inordinately high concentrations of impurities relative to the bulk of the layers, so that it is natural that the scattering is stronger than in the bulk of the layers.

* Corresponding author. Email: levy@acf3.nyu.edu; fax: +1-212-995-4016.

PII S0304-8853(96)00436-2

In the transition-metal magnetic multilayers that have been grown over the past eight years there are two principal geometries for measuring magneto-transport properties; current in the plane of the layers (CIP), and current perpendicular to the plane of the layers (CPP). There are several reviews on the giant magnetoresistance in these geometries [3,4]. Here we review recent calculations of these transport properties, what the approximations are, how we account for vertex corrections when using impurity averaged propagators, the role of band structure and potential steps in the transport, and the meaning of the electric fields we introduce to calculate the CPP transport.

2. Diffusive transport

Two artifices are introduced to calculate transport properties of electron systems in the diffusive regime: internal fields and vertex corrections.

2.1. Internal fields

The conductivity we calculate usually relates current to an 'internal or local' field in a solid. As transport calculations are based on one electron Hamiltonians, the Coulomb interaction between electrons is accounted for in a mean field sense (Hartree field); this produces the distinction between externally applied fields and internal fields. In the random phase approximation (time-dependent Hartree–Fock) Coulomb interactions between itinerant electrons are represented by polarization diagrams that renormalize the field acting locally on the electrons. We will not be interested in variations of this field on atomic length scales; rather we are interested in variations on the scale of several lattice constants. It follows that for magnetic multilayers this internal field is the same for applied fields parallel and perpendicular to the layers, as long as the fields are applied along equivalent direction of the underlying atomic lattice.

2.2. Vertex corrections

Transport calculations occurs in two broad regimes. In ballistic transport either there is no scattering in the sample (rather it takes place in the reservoirs), or for a small number of scatterers one keeps track of the scattering *amplitudes* and calculates the propagators for a specific distribution of scatterers. In the ballistic regime one can calculate the conductance exactly by using the Landauer–Buttiker approach [5], or one can calculate the conductance of a system with a small number of impurities, repeat the calculation for different realizations of the impurity distributions, and then take the average of these to find the conductivity [6]. In both approaches, the propagators for the actual potentials are used, i.e., there is no impurity averaging *before* one calculates the conductivity, so that there are no vertex corrections from impurity averaging to be taken into account.

For diffusive transport scattering is frequent, and calculating exact propagators for these densities of scatterers is intractable. In these cases one resorts to impurity averaged propagators in which one does not retain the phase information from one scattering center to another. However, transport is sensitive to some of these phases, and vertex corrections are introduced to account for them and to properly calculate the conductivity [7]. For example vertex corrections are needed to distinguish between the life-time of an electron due to scattering, and its *transport* life-time as it enters the Boltzmann equation.

For ab-initio calculations of the resistance in the diffusive regime one should definitely start with correct wavefunctions of the superlattice, which are Bloch states, and self-consistently calculate the effects of the defect and impurity scattering on the band structure. This is usually done in the coherent potential approximation (CPA). The result from such a determination is an electronic structure which cannot be classified by momentum eigenstates of the superlattice. Rather what's left is best described by Bloch spectral distribution functions [8], i.e., the quasi-particle description of the electron states may well break down. In this limit there is a well defined procedure for calculating the conductivity based on the Kubo formalism that has been used for random alloys [9]. An advantage of this approach over the Boltzmann formalism is that one does not have to constrain the variables of integration to the Fermi surface. This condition is enforced by a sort of Lagrangian multiplier, because energy and momentum are independent variables in the Kubo approach which uses Green's functions [7].

3. CIP and CPP transport

With the relation of current to internal field it is straightforward, if tedious, to calculate the conductivity or resistivity that's measured on multilayered structures. While there are always vertex corrections from impurity scattering to the non-local two point conductivity tensor $\sigma(\boldsymbol{r},\boldsymbol{r}')$, we distinguish between two types of corrections. The first one is the vertex correction which is due to momentum dependent self-energy; this type of vertex exists in homogeneous systems which we are not interested here. In order to exclusively study vertex corrections that are induced by the inhomogeneity of the structure (layering), we choose scattering to be short-ranged so that the first type of vertex correction disappears. For layered structures, the fundamental object is the conductivity tensor $\sigma(z,z') = \int \mathrm{d}x\mathrm{d}y\,\sigma(\boldsymbol{r},\boldsymbol{r}')$ where z is the direction of layer growth. Since layered structures are assumed to be homogeneous in the plane of the layer, the impurity averaged Green's function is translational invariant in the plane of the layer, i.e., $G(\boldsymbol{r},\boldsymbol{r}') = G(\rho-\rho',z,z')$. It is convenient to work in mixed momentum ($\boldsymbol{k}_\parallel$) and coordinate representations (z); one can write the conductivity tensor by summing over all the ladder diagrams,

$$\sigma_{\mathrm{CIP}}(z,z') \propto \sum_{\boldsymbol{k}_\parallel} \boldsymbol{k}_\parallel^2 G(\boldsymbol{k}_\parallel,z,z')G(\boldsymbol{k}_\parallel,z,z') + \sum_{\boldsymbol{k}_\parallel\boldsymbol{k}'_\parallel,z_1} (\boldsymbol{k}_\parallel\cdot\boldsymbol{k}'_\parallel)G(\boldsymbol{k}_\parallel,z,z_1) \times G(\boldsymbol{k}_\parallel,z,z_1)\Gamma(z_1)G(\boldsymbol{k}'_\parallel,z_1,z') \times G(\boldsymbol{k}'_\parallel,z_1,z') + \cdots \tag{3.1}$$

and

$$\sigma_{\mathrm{CPP}}(z,z') \propto \sum_{\boldsymbol{k}\parallel} G(\boldsymbol{k}_\parallel,z,z')\frac{\partial}{\partial z}\frac{\partial}{\partial z'}G(\boldsymbol{k}_\parallel,z,z') + \sum_{\boldsymbol{k}_\parallel\boldsymbol{k}'_\parallel,z_1} G(\boldsymbol{k}_\parallel,z,z_1)\frac{\partial}{\partial z}G(\boldsymbol{k}_\parallel,z,z_1) \times \Gamma(z_1)G(\boldsymbol{k}'_\parallel,z_1,z')\frac{\partial}{\partial z'}G(\boldsymbol{k}'_\parallel,z_1,z') + \cdots \tag{3.2}$$

where the scattering vertex $\Gamma(z_1)$ only depends on the z coordinate (independent of momentum $\boldsymbol{k}_\parallel$) since we assumed short range scattering potentials. The first terms in Eqs. (3.1) and (3.2) are the bubble diagrams for CIP and CPP. The remaining terms are contributions from the ladder diagrams to the conductivity tensor; we have neglected other diagrams, e.g., maximally crossed diagrams for localization effects. The terms other than the first in Eq. (3.1) vanish because summations over parallel momenta in the vertex terms are over odd functions of the momentum variables and are zero. Therefore, if the scattering potential is short-range we conclude that the CIP conductivity is solely determined by the bubble diagram; this makes the calculation for CIP conductivity simpler than that for CPP. The disappearance of vertex corrections in CIP has a straightforward consequence: there is no charge or spin accumulation for transport parallel to the layers, as long as the layers are homogeneous and do not contain grains or domains. This approximation is good for impurities in the bulk of the layers; however, when we account for the extended scattering at interfaces this approximation breaks down and vertex corrections appear from interface scattering for CIP.

On the contrary, vertex corrections contribute to the CPP conductivity $\sigma_{\mathrm{CPP}}(z,z')$ irrespective of the range of the scatterers; as one sees from Eq. (3.2) vertex corrections exist. This requires us to calculate them term by term in Eq. (3.2), which is highly non-trivial work. Except for special cases [6] Eq. (3.2) is intractable in inhomogeneous medium. However, the interpretation of these vertex corrections is transparent, i.e., they represent the charge and spin accumulation in the presence of inhomogeneous spin-dependent scattering. In the next section, we will focus our review on CPP transport.

To summarize, as long as we do not account for the extended nature of the scattering at interfaces, the bubble (no vertex corrections) CIP conductivity suffices for CIP; for the CPP geometry vertex corrections are always needed.

4. Effective fields

In ab-initio or model calculations of the CPP transport there are two ways in which vertex correc-

tions can be accounted for. Either to explicitly calculate them, as has been done in some simplified model calculations [6], or to go the route of effective fields, i.e., to stay with the bubble diagram for the conductivity and invoke an effective field to satisfy current conservation in each 'spin channel'. The mathematical advantage of the second method is that one avoids calculating the vertex terms in Eq. (3.2) for the CPP transport. We now show the equivalence of these two methods.

The effective field is defined as [10]

$$E^s_{\mathrm{eff}}(z') = \int \rho^s_{\mathrm{b}}(z', z_1)\, \sigma^s(z_1, z_2)\, E(z_2)\, \mathrm{d}z_1\, \mathrm{d}z_2, \tag{4.1}$$

where σ^s is the conductivity Eq. (3.2) for one spin channel s, $\rho^s_{\mathrm{b}}(z', z_1)$ is the inverse of the bubble conductivity $\sigma^s_{\mathrm{b}}(z, z')$ (the first term in Eq. (3.2)), and we have dropped the label for CPP. Notice that the effective field is spin dependent because both the conductivity tensor and the 'bubble' resistivity tensor are spin dependent. The linear response is now written as

$$j^s(z) = \int \sigma^s_{\mathrm{b}}(z, z')\, E^s_{\mathrm{eff}}(z')\, \mathrm{d}z'. \tag{4.2}$$

By substituting Eq. (4.1) into Eq. (4.2), we can easily verify that it is equivalent to the original linear response relation

$$j^s(z) = \int \sigma^s(z, z')\, E(z')\, \mathrm{d}z'. \tag{4.3}$$

A physical constraint on the vertex corrections in Eq. (3.2) is that the conductivity tensor must be divergenceless, i.e., $(\partial/\partial z)\sigma^s(z, z') = 0$ [11], so that the current conservation is guaranteed for Eq. (4.3). By integrating Eq. (4.3) by parts, one finds the measured conductivity is given by

$$\sigma_{\mathrm{CPP}} = \sum_s \int \sigma^s(z, z')\, \mathrm{d}z\, \mathrm{d}z', \tag{4.4}$$

which is independent on the detail of the internal field $E(z')$, provided one uses correct $\sigma^s(z, z')$ [11]. However, the calculation of the full conductivity tensor σ^s, Eq. (3.2), is usually difficult. Our introduction of the effective field, Eq. (4.1), supplies an alternate and efficient way to calculate the measured conductivity as we will show below.

While the bubble conductivity $\sigma^{\mathrm{b}}(z, z')$ is easier to obtain, it does not possess the property of being divergenceless as the full conductivity does. One can verify this by a direct calculation [10]. Therefore the measured conductivity will depend on the detail of the effective field. The central problem of the CPP transport is to evaluate the effective field in this approach.

The determination of the effective field relies on the principle of the current conservation. Since linear response, Eq. (4.2), is one-dimensional, current conservation ($(\partial/\partial z) j^s(z) = 0$) leads to a constant current j^s for each spin channel (we neglect spin-flip processes) and the effective field is simply $E^s_{\mathrm{eff}}(z) = j^s \int \rho^s_{\mathrm{b}}(z, z')\, \mathrm{d}z'$.

Two questions arise regarding the effective field we introduced. First, the relation of these spin-dependent effective fields to the external or internal electric fields used in the more conventional formulations of the conductivity. If the medium is homogeneous, one can easily show that the effective field is same as the internal field [11]; therefore there is no spin-dependence of the field. In inhomogeneous media, the effective fields vary spatially. The difference between the effective field and the internal field describes charge and spin accumulation in inhomogeneous media. Formally, we can introduce the spin-dependent voltage drop $V^s(z) = \int_0^z E^s_{\mathrm{eff}}(z')\, \mathrm{d}z' = j^s \int_0^z \mathrm{d}z' \int \rho^s_{\mathrm{b}}(z', z'')\, \mathrm{d}z''$. When the voltage probe is placed across the sample with length L, the boundary condition requires $V^s(L) = V$, where V is the voltage across the sample which is spin-independent; this boundary condition is used to determine the spin-dependent constant current j^s. Finally, the total conductivity is obtained via the two current model, $\sigma_t = \sum_s j^s / V$.

The second question is whether there is a way to measure these fields. Since these effective fields are defined in terms of vertex corrections, Eq. (4.1), they are not directly measurable. However, an indirect measurement can, in principle, be performed. For example, the spin injection-detection experiment [12] measures the spin-dependent chemical potentials which are the integration of the effective fields. Here we outline an experiment that further illustrates the role of these effective fields.

In Fig. 1, a spin-polarized current flows through the sample in z-direction. A probe is attached to

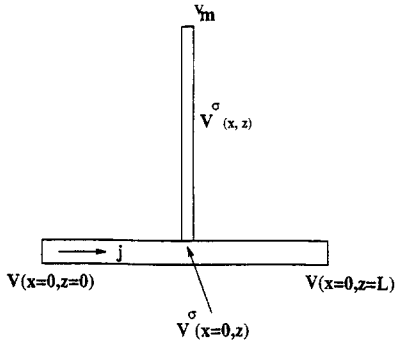

Fig. 1. Geometry for the measurement of spin-dependent effective fields at position z.

measure the voltage at any point z. Let us assume that we are able to determine the effective field at point z along the sample, i.e., $E^s_{\text{eff}}(x=0,\ z) = j^s \int \rho^s_b(z,\ z')\,dz'$, or $V^s(x=0,\ z) = \int_0^z E^s_{\text{eff}}(x=0,\ z')\,dz'$. The measured potential at the end of the probe is then $V_m = V^s(x=\infty,\ z)$, and it is independent of spin [13]. The current-field relation for each spin channel in the probe is

$$j^s(x,z) = \sigma_p^s \frac{\partial}{\partial x} V^s(x,z), \tag{4.5}$$

where σ_p^s is the conductivity of the probe which is assumed to be uniform but may depend on the spin. Since the total current in the probe is zero as required by the open circuit boundary condition, i.e., $\sum_s j^s(x,z) = 0$, we find, from Eq. (4.5),

$$\sigma_p^{\uparrow} V^{\uparrow}(x,z) + \sigma_p^{\downarrow} V^{\downarrow}(x,z) = C, \tag{4.6}$$

where C is a constant. By applying the above equation to two points, $x=0$ and $x=\infty$, one arrives at

$$V_m = \frac{\sigma_p^{\uparrow} V^{\uparrow}(x=0,z) + \sigma_p^{\downarrow} V^{\downarrow}(x=0,z)}{\sigma_p^{\uparrow} + \sigma_p^{\downarrow}}. \tag{4.7}$$

If one uses a non-magnetic probe so that $\sigma_p^{\downarrow} = \sigma_p^{\uparrow}$, the measured potential is simply the average of the spin-dependent potential, i.e., $V_m = (V^{\uparrow}(x=0,\ z) + V^{\downarrow}(x=0,\ z))/2 \equiv \bar{V}$. If one uses a ferromagnetic probe, one finds

$$V_m = \bar{V} + P\Delta V/2, \tag{4.8}$$

where P is the polarization of the ferromagnetic probe $P = (\sigma_p^{\uparrow} - \sigma_p^{\downarrow})/(\sigma_p^{\uparrow} + \sigma_p^{\downarrow})$ and $\Delta V = V^{\uparrow}(x=0,z) - V^{\downarrow}(x=0,z)$. This illustrates that, by using a ferromagnetic probe, one can detect the spin accumulation ΔV; it is the same idea which has been carried out in spin injection-detection experiments [12].

By using this effective approach we have been able to show that in the limit where the mean free path of the electrons is small compared to the thicknesses of the layers the measured resistance for CIP is given as a sum of the local conductivities, while for CPP it is the sum of the local resistivities, i.e., resistor network analogies are applicable in this limit, so that in CIP the multilayer acts as resistors in parallel do, and for CPP as resistors in series [14]. These analogies are rather transparent if we use effective fields to assure current conservation when we do not include vertex corrections for the conductivity.

While the above resistor network analogy may seem obvious or intuitive, it has been shown that the measured resistance or conductance is a sum over the correct non-local conductivity tensor irrespective of the internal electric field, i.e., this must hold for CPP as well as CIP [6]; see Eq. (4.4). While the resistor network analogy seemingly contradicts this, the conundrum is resolved by recognizing that the correct conductivity tensor for CPP contains vertex corrections, which if neglected, must be compensated for by adding bubble diagram resistivities rather than the full conductivities.

Although the spin and range dependence of these effective fields are not essential to the determination of the measured resistivity (conductivity), they are nonetheless interesting, because they are directly related to the spin dependent chemical potentials that are produced when current is driven across regions with different spin-dependent scattering. These fields or potentials have been related to the spin accumulation attendant to charge transport, i.e., to the current driven magnetization. As we have previously shown in the limit where the mean free path of the electrons is short compared to the thickness of the layers, this effective field is directly proportional to the local scattering. Simply put, this is the way one maintains current conservation in an inhomogeneous system when the scattering is varying from one region to another. For inhomogeneous magnetic structures with negligible spin diffusion we need *separate* effective

fields to conserve current for each of the independent up and down spin channels, and we arrive at the concept of spin-dependent fields. The spatial dependence of these fields is controlled by the diffusion propagators as we have shown elsewhere [10].

5. Band structure

Recently there have been a series of studies that have stressed the role of the electronic band structure of the multilayer in producing different conductivities and magnetoresistance for current parallel and perpendicular to the layers, when *only* contributions from bubble diagrams are taken into account [15]. When the effect of impurity and defect scattering on the electronic structure is taken into account we find that the transport properties of the transition-metal multilayers are governed by features of the multilayers that are limited to the mean free path of the conduction electrons due to momentum relaxing processes [16]. In other words, except for inordinately thin layers (of the order of 5–10 Å) and very clean samples, the superzone band gaps, due to the periodic potential of the superlattice (coherent scattering from the putative potential steps at interfaces between dissimilar metals), do not enter the calculation of the conductivity (of course the gaps from the periodicity of the atomic potentials do enter). Once superzone gaps do not enter the conductivity there is little difference between the CIP and CPP conductivities and magnetoresistance that arise from the band structure if these materials are cubic, and if the currents are along equivalent symmetry directions of the atomic lattice. Therefore, it is the vertex corrections discussed in Section 3 that are responsible for the differences between CIP and CPP.

To further quantify the above argument we use a simple model to determine the role of superlattice superzone boundary gaps on the conductivity in the presence of impurity scattering. The model consists of a one dimensional Kronig–Penney potential with wells V_a, barriers V_b, and the Fermi energy at E_F. The dispersion relation for this simple model is

$$\epsilon_k = \cos(k_a a)\cos(k_b b) + \frac{k_a^2 + k_b^2}{2k_a k_b}\sin(k_a a)\sin(k_b b), \tag{5.1}$$

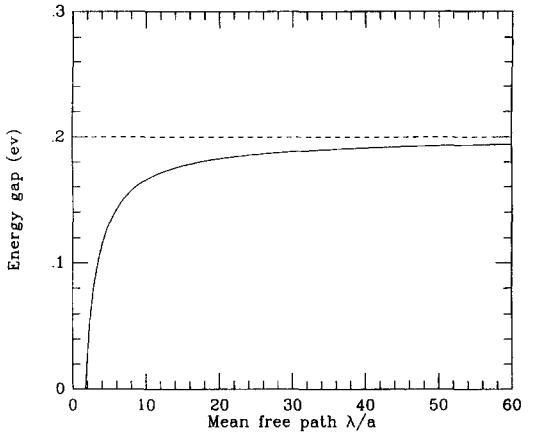

Fig. 2. Band gap as a function of the mean free path. The dotted line is the gap size without disorder calculated by using Eq. (5.1) with equal thickness of all the layers ($a = b = 20$ Å). We have chosen $k_a a = 60$ and $k_b b = 40$.

where a and b are the thicknesses of the layers for the wells and barriers, and $k_i = \sqrt{2m(\epsilon - V_i)}/\hbar$ ($i = a, b$). Eq. (5.1) determines the gaps and bands. Now let us introduce disorder to the system; the scattering from the disorder (impurities) leads to uncertainty in the phases of electrons as they travel from one interface to the next. This uncertainty can be quantified statistically in terms of the mean free path, i.e., $\phi_a = 2\pi a/\lambda_a$, where ϕ is the uncertainty of the phase difference across a well (barrier). From calculations similar to those used to arrive Eq. (5.1), we find in the presence of disorder,

$$\epsilon_k = \cos(k_a a + \Delta\phi_a)\cos(k_b b + \Delta\phi_b) + \frac{k_a^2 + k_b^2}{2k_a k_b}\sin(k_a a + \Delta\phi_a)\sin(k_b b + \Delta\phi_b), \tag{5.2}$$

where $\Delta\phi_i$ is a random variable within the uncertainty ϕ_i defined above. In a perfect superlattice (no scattering) the band edge is sharp and well-defined, i.e., all energies which are (are not) solutions of Eq. (5.1) determine the bands (gaps). When disorder exists, some of the gap states becomes band states, i.e., an energy which is not the solution of Eq. (5.1) is a solution of Eq. (5.2) due to the phase shift caused by scattering. This is precisely the effect of smearing of the superlattice bands. To estimate the onset of the disappearance of the gap states, we

focus on an original gap $E_g = \epsilon_h - \epsilon_l$, where ϵ_h and ϵ_l are high and low energies of the gap, i.e., the energy in the gap satisfies

$$k_a(\epsilon_l)a + \phi_a < k_a(\epsilon)a < k_a(\epsilon_h)a - \phi_a, \qquad (5.3)$$

a similar relation applies to the barriers. Clearly the gap disappears when $k_a(\epsilon_h)a - k_a(\epsilon_l)a < 2\phi_a$. In Fig. 2, we show an example of the gap size as function of the mean free path. For superzone gaps to be clearly seen in the presence of disorder, the mean free path should be about ten times greater than layer thickness $(a + b)$.

Here we want to stress that contributions from vertex corrections to CPP transport are not conditioned on whether the transport in the transition-metal multilayers is ballistic or diffuse; they always appear. However, we have just shown that the differences between CPP and CIP conductivities due to the electronic structure of the superlattice are predicated on the condition that the mean free paths in these multilayers are long enough for the transport to be sensitive to the coherent scattering from successive potential steps that produce the superzone Brillouin zone gaps in the electronic structure. At the present time this does not appear to be true, and we believe that for the diffusive transport in the transition-metal multilayers that display GMR, the difference between the CIP-MR and CPP-MR is primarily due to vertex corrections and *not* the superlattice band structure.

Finally we wish to comment on the role of quantum well effects when systems are truly ballistic (a goal not yet attained experimentally, but may be reached in the future). The superlattice band structures are indeed playing important roles in determining the magnetotransport properties. One conceivable phenomenon is the oscillatory behavior in the conductivity and magnetoresistance. Currently, most effects due to quantum wells have been discussed for the CPP geometry [17]. We want to emphasize that quantum well effects are actually more pronounced in CIP than in CPP for the following reason. In the CIP geometry, the major contribution to the conductivity comes from states with large parallel momenta $(\boldsymbol{k}_\parallel)$. Therefore the energy in the growth direction $\epsilon_z = E_F - \epsilon_{\mathbf{k}_\parallel}$ is small, and CIP favors states *deep* in the wells, in which quantum well effects or superzone gaps are most pronounced.

6. Potential steps

There have been suggestions that potential steps (steps in the potential that model differences in the electronic properties of the layers) at interfaces by themselves (no roughness) are sources of resistance for CPP [19]. To clarify how the resistance is affected by the presence of the potential steps, we consider two distinct cases, ballistic and diffusive, separately. In the ballistic region, one calculates the conducting (itinerant) states in the perfect superlattice with these spin dependent steps, and one is able to use Landauer's formula to connect the resistance of the system to the transmission probability of these conducting states. Schep et al. [5] have illustrated that one can obtain a large magnetoresistance *ratio* merely from this spin-dependent contact resistance.

In the diffusive region, one can *not separate* the resistivity coming from potential steps and diffusive scattering into two parts in general. One may define the resistance from the potential steps as

$$\Delta R = R(\text{step}) - R(0), \qquad (6.1)$$

where R(step) and $R(0)$ are the resistance with and without potential steps; this definition has been implicitly adopted by those working on models of GMR in the diffusive regime [2,18]. Here we should discuss two limiting cases, homogeneous and local limits.

In the homogeneous limit where the mean free path is much larger than the layer thickness, one would calculate the electronic structure with potential steps first, and treat the impurity scattering as a perturbation. Since both R(step) and $R(0)$ are proportional to the scattering parameters, we conclude that the resistance from potential steps ΔR is indeed dependent on the scattering rates in the bulk.

In the local limit where the mean free path is much smaller than the layer thickness, it has been shown by Barnas and Fert [19], Dugaev et al. [20], Vedyaev et al. [21], and Stiles [22] that ΔR can be solely determined by the reflection coefficients at potentials steps, i.e., independent of the scattering in the bulk. Therefore it is meaningful to single out the resistance of the potential steps from that of total. We have examined the difference in the contributions to the resistance for CPP coming from the coherent scattering at the interfaces from potential

steps, and from the diffuse scattering in the bulk of the layers. The details of this will be published elsewhere.

In ab-initio calculations, it is rather straightforward to calculate resistance in the presence of potential steps: one calculates the band structure self-consistently which includes the effect of impurity scattering, and uses linear response theory (Kubo formalism) to arrive at conductivity and magnetoresistance. Similarly, in model calculations, one assumes spin-dependent potential steps and relaxation times at interfaces and in the bulk. For example, Hood et al. [2] calculated the magnetoresistance in the presence of potential steps for the CIP geometry. From their results, the magnetoresistance does indeed change as one varies the height of potential steps.

7. Conclusions

To calculate the measured resistance in the CIP geometry it is sufficient to calculate the local conductivity tensor by considering only contributions from bubble diagrams that consist of uncorrelated impurity-averaged electron hole propagators, and then by summing these local conductivities to arrive at the measured conductivity or its inverse the resistivity.

$$\sigma_{\mathrm{CIP}} = \rho_{\mathrm{CIP}}^{-1} = \sum_{s} \frac{1}{L} \int \sigma_{\mathrm{CIP}}^{s}(z, z')\, \mathrm{d}z\, \mathrm{d}z'. \qquad (7.1)$$

For CIP transport the additional contributions to the local two-point conductivity from vertex corrections cancel out. For the CPP geometry it is *in*sufficient to consider only bubble diagrams; vertex corrections contribute to this geometry, i.e., they do not vanish as we have shown for CIP.

How we think or model transport in magnetic multilayers may be different from how we should calculate the transport. In developing an understanding of the differences between CIP *and* CPP transport it is useful to introduce the concept of spin-dependent electric fields that vary from one layer to the other. This naturally invokes the idea that charge transport across regions of varying spin-dependent scattering, i.e., CPP, produces spin-dependent chemical potential build-ups with a concomitant current driven or non-equilibrium magnetization. These are real effects and produce the differences between CIP and CPP transport that have been observed. The fact that there is a superlattice band structure, which may play some role in producing differences between CIP and CPP transport, is very much in the background in models where such differences are mainly attributed to current driven effective field effects. As these field or chemical potential effects are not predicated on the mean free path being long enough compared to the thicknesses of the layers, they are 'robust' and will always produce differences between CIP and CPP transport; in fact the differences grow as the mean free path becomes small compared to the thicknesses of the layers. On the contrary effects of the superlattice potential (Section 5) are predicated on the mean free path being large compared to the layer thicknesses; they are fragile, inasmuch as this condition is *not* met in most of the multilayers that display GMR, so that the differences due to superlattice band structure disappear.

We can summarize the current status as follows:

In the limit where the mean free path of the electrons is large compared to the thickness of the layers, one has the concept of 'self-averaging', i.e., the global resistivity does not depend on the detail of the layering which is in analogy to the case that the detail impurity distribution is not important in bulk metallic materials. In this case our effective fields do *not* produce differences between CIP and CPP transport, however the superlattice band structure does produce differences. Also in this case Bloch functions for the superlattice are appropriate for describing the transport.

For the opposite limit, where mean free paths are shorter than the thickness of the layers, the superlattice band structure does *not* produce differences between CIP and CPP transport, but the vertex corrections most assuredly will. Another source to produce the difference is the contribution from potential steps at interfaces for CPP transport.

Therefore the relative importance to CPP-MR of superlattice band structure compared to the vertex corrections depend on the conditions of transport in the transition-metal magnetic multilayers in which GMR has been observed. From our fits to the data, as well as those by the experimental groups [23], we find reality is closer to mean free paths that are

comparable to the thickness of the layers. Therefore, at the present time we conclude that it is the spin and charge accumulation (vertex corrections) that are the primary origin for the differences between CPP and CIP transport.

Acknowledgements

One of the authors (P.M. Levy) would like to thank the Japan Society for the Promotion of Science for the opportunity to visit several research institutions in Japan. It was in the course of probing discussions with Professors S. Maekawa, J. Inoue, H. Fujimori, T. Shinjo and H. Sato, and with Dr. H. Itoh that the questions addressed in this review arose. The authors wish to thank Dr. M. Stiles and Prof. A. Fert for helpful discussions. This work is supported by Office of Naval Research grant through N00014-96-1-0203.

References

[1] M.B. Stearns, J. Magn. Magn. Mater. 104–107 (1992) 1745.
[2] R.Q. Hood, L.M. Falicov and D.R. Penn, Phys. Rev. B 49 (1994) 368; R.Q. Hood and L.M. Falicov, Phys. Rev. B 46 (1992) 8287.
[3] P.M. Levy, Solid State Physics, Vol. 47, eds. H. Ehrenreich and D. Turnbull (Academic Press, Cambridge, MA, 1994) pp. 367–462.
[4] M.A.M. Gijs and G.E.W. Bauer, Adv. Phys., to be published.
[5] K.M. Schep, P.J. Kelly and G.E.W. Bauer, Phys. Rev. Lett. 74 (1995) 586; G.E.W. Bauer, K.M. Schep and P.J. Kelly, J. Magn. Magn. Mater. 151 (1995) 369.
[6] H. Itoh, J. Inoue and S. Maekawa, Phys. Rev. B 51 (1995) 342.
[7] G.D. Mahan, Many-Particle Physics (Plenum, New York, 1981).
[8] P. Weinberger, Electron Scattering Theory for Ordered and Disordered Matter (Clarendon Press, Oxford, 1990).
[9] W.H. Butler, Phys. Rev. B 31 (1985) 3260; J. Banhart, H. Ebert, P. Weinberger and J. Voitlander, Phys. Rev. B 50 (1994) 2104.
[10] H.E. Camblong, P.M. Levy and S. Zhang, Phys. Rev. B 51 (1995) 16052.
[11] C.L. Kane, R.A. Serota and P.A. Lee, Phys. Rev. B 37 (1988) 6701.
[12] M. Johnson, Appl. Phys. Lett. 63 (1993) 1435.
[13] We assume that the length of the probe is longer than the spin-diffusion length in the probe. By using the diffusion equation, see T. Valet and A. Fert, J. Magn. Magn. Mater. 121 (1993) 378; Phys. Rev. B 48 (1993) 7099, we obtain $V^{\uparrow}(x,z) - V^{\downarrow}(x,z) = A\exp(-x/D)$, where D is the diffusion length. For $x \gg D$, $V^{\uparrow}(x,z) = V^{\downarrow}(x,z) = V_m$ which is independent of the spin.
[14] H.E. Camblong, S. Zhang and P.M. Levy, Phys. Rev. B 47 (1993) 4735.
[15] I. Mertig et al., J. Magn. Magn. Mater. 151 (1995) 363.
[16] P.M. Levy and S. Zhang, J. Magn. Magn. Mater. 151 (1995) 315.
[17] J. Mathon, M. Villeret and H. Itoh, Phys. Rev. B 52 (1995) 6983.
[18] S. Zhang and P.M. Levy, Magnetic Ultrathin Films, ed. B.T. Jonker et al., MRS Symp. Proc. 313 (1993) 53.
[19] J. Barnas and A. Fert, Phys. Rev. B 49 (1994) 12835; A. Fert, T. Valet and J. Barnas, J. Appl. Phys. 75 (1994) 6693.
[20] V.K. Dugaev, V.I. Litvinov and P.P. Petrov, Phys. Rev. B 52 (1995) 5306.
[21] A. Vedyaev, C. Cowache, N. Ryzhanova and B. Dieny, Phys. Lett. A 198 (1995) 267.
[22] M. Stiles, private communication; and J. Appl. Phys. 79 (1996) 5805.
[23] S.-F. Lee et al., Phys. Rev. B 46 (1992) 548; M.A. Gijs et al., J. Appl. Phys. 75 (1994) 6709.